

UNCLASSIFIED

Q #2176 Q12

CONTROL SYSTEMS LABORATORY

A NEW TYPE OF ELECTRIC DELAY LINE

Report R-80

March 1956

Numbered Pages: 48

Contract DA-11-022-ORD-174

UNIVERSITY OF ILLINOIS · URBANA · ILLINOIS

UNCLASSIFIED

"The research reported in this document was made possible by support extended to the University of Illinois, Control Systems Laboratory, jointly by the Department of the Army (Signal Corps and Ordnance Corps), Department of the Navy (Office of Naval Research), and the Department of the Air Force (Office of Scientific Research, Air Research and Development Command), under Signal Corps Contract DA-36-039-SC-56695, Project 8-103A, D/A Project 3-99-10-101."

UNCLASSIFIED

80-1

Report R-80

A NEW TYPE OF ELECTRIC DELAY LINE

Prepared by:
Leo Lavatelli

March 1956

CONTROL SYSTEMS LABORATORY
UNIVERSITY OF ILLINOIS
URBANA, ILLINOIS
Contract DA-11-022-ORD-174

Numbered Pages: 48

UNCLASSIFIED

ABSTRACT

This report discusses briefly the design of an experimental model of a delay line, which exploits the motion of electrons in crossed electric and magnetic fields. The results of preliminary measurements are presented and analyzed. The most encouraging result is the delay of about 100 microseconds over a one inch transit space.

FOREWORD

The device discussed in this report was conceived in the period immediately preceding the formal establishment of the Control Systems Laboratory. At that time the program of the Laboratory was being formulated, and it later became apparent that component development of this nature should be accorded a secondary status in terms of time and personnel. As the pressure of the primary programs increased it was necessary to suspend the experimental investigation of the delay line. It was the hope of the author that work could be resumed at a later time and for this reason the publication of the investigation was delayed until a more definite statement regarding feasibility could be made. It is now apparent that no further work on the device can be undertaken, and therefore this report is published without a complete understanding of the behavior of the device and without being able to answer completely the question of feasibility.

It is a pleasure to acknowledge the friendly interest and assistance of Professor David Lazarus in all phases of this work, and the helpful discussions with many members of the staff of the Control Systems Laboratory.

TABLE OF CONTENTS

	Page
Abstract	3
Foreword	5
Table of Contents	7
List of Illustrations.	9
I. Introduction	11
II. Electron Motion in Crossed Fields.	12
III. Focussing	14
IV. Experimental Delay Line.	15
V. Results.	24
VI. Discussion.	27
Appendix I Motion of a Charged Particle in Various Static Fields.	35
Appendix II Calculation of the Electric Field.	43

LIST OF ILLUSTRATIONS

	Page
Figure 1. Decomposition of the Trochoidal Orbit into Pure Rotation and Pure Translation	13
Figure 2. Schematic Representation of the Delay Line Field Geometry.	16
Figure 3. Interior View of Chamber and Magnet	17
Figure 4. Chamber Interior	18
Figure 5. Source with Shield Removed	20
Figure 6. Source Detail	21
Figure 7. Chamber Detail	22
Figure 8. Circuit Schematic	23
Figure 9. Radial Plot of Magnetic Field Intensity on Median Plane.	25
Figure 10. Waveform of Collector Signal and Tabulated Delay Times Versus Center Plate Voltage	26
Figure 11. Graph of Results	30
Figure 12. Two Dimensional Representation of Chamber.	44
Figure 13. Mapping of the Chamber Interior on the Upper Half-Plane.	45
Figure 14. Plot of the Components of the Fringing Field on a Plane 1 mm. above the Center Plate.	48

A New Type of Electric Delay Line

I. Introduction

Nearly all the delay devices used in modern radar and digital computers have the disadvantage of either being bulky, or else requiring auxiliary circuits of considerably complexity. These components include mercury and quartz acoustical delay lines, storage tubes, magnetic drums, magnetic core memories, spin echo memories as well as the conventional delay lines of either the distributed or lumped constant type. Only the latter type is passive in nature, requiring no additional circuits for its use, but this type can only give delays of the order of microseconds before its bulk renders it too inconvenient for practical use.

The delay line discussed in this report uses the time of flight of electrons over a fixed transit space as the basic delay mechanism. A practical dimension to consider for the length of the transit space is the width of standard relay racks, say 50 centimeters. Useful delay times for computers are about 50 microseconds; for MTI radar: 5000 microseconds. If electron transit times over straight line trajectories are used as the delay mechanism, then for a 50 cm. transit space the electron velocities corresponding to these times, are 10^6 cm/sec and 10^4 cm/sec, and the corresponding electron energies are 0.0003 and 0.00000003 electron volts, respectively. To obtain high resolution of the input pulses at the output requires a monoenergetic beam, but it is difficult to produce such beams with these low energies, and furthermore, such beams are easily perturbed by weak electric and magnetic fields. These difficulties are avoided in the present device by using the motion of electrons in crossed electric and magnetic fields. Preliminary tests of the experimental model described below indicated that satisfactory performance could be achieved without critical adjustment of the available parameters, in fact, signal velocities about 5 times slower than mercury delay lines were obtained.

The basic delay mechanism considered in this report is the drift motion of electrons in crossed electric and magnetic fields. The drift velocity is independent of the energy, mass, and the

sign of the charge of the particles and depends only on the ratio of the electric to magnetic field strengths. It is easy to adjust this ratio to give velocities 10^4 times smaller than the path velocity of a 50 volt electron and 10 times smaller than the velocity of the acoustic pulses in conventional sonic delay lines. Furthermore, since the velocity is independent of energy, it should be possible, in principle, to achieve long delays with very wide band response. One fact militates against realizing this very large bandwidth; when the fields are uniform, there is no focussing force to keep the particles from diffusing in directions parallel to the magnetic field. If one attempts to use an electric field shape to give focussing, the component of the field at right angles to the magnetic field is no longer uniform and therefore a velocity spread across the beam is automatically guaranteed, thus reducing the bandwidth. However, by suitably trading bandwidth for focussing a practical device seems feasible to build. The device described below was not intended to be any more than a preliminary model to be used to test various source designs. The ease and stability of its initial performance was very encouraging.

II. Electron Motion in Crossed Fields

The motion of electrons in crossed fields can be shown to consist of uniform circular motion plus a uniform translational velocity at right angles to the electric and magnetic field directions. See Figure 1 and Appendix I. The translational velocity depends only on the ratio of the electric to the magnetic field strengths. As a consequence, the electron energies in the delay line can be the same as in common vacuum tubes, i.e. 10 to 100 electron volts. The energies need not be mono-energetic, since the translational drift velocity is independent of the particle energies. As is shown in Appendix I, the drift velocity in cm/sec is $v_d = 10^8 E/H$ with E in volts/cm and H in gauss. If H is produced by a permanent magnet, the ratio, E/H can be adjusted easily by changing the potential of one electrode. Thus translational velocities in the range of 10^4 to 10^6 cm/sec

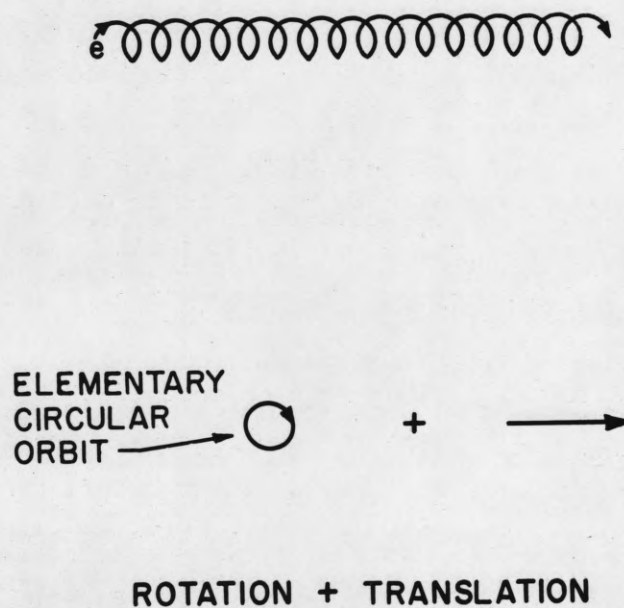


FIG. 1 DECOMPOSITION OF THE TROCHOIDAL ORBIT INTO PURE ROTATION AND PURE TRANSLATION.

are easily achieved using magnetic fields of the order of kilograms and electric fields of the order of volts/cm.

III. Focussing

The above considerations hold rigorously only if the fields are uniform. In this case there is no preferred plane in which the above motion occurs. That is, if the electrons possess any component of velocity parallel to the magnetic field, this velocity will remain unchanged, because no force acts in this direction. Since it is difficult to produce a beam of electrons with no angular divergence, this lack of a focussing force makes it difficult to design a delay line in which all of the current leaving a source is received at the collector.

The magnetic focussing that is used in cyclotrons and betatrons cannot be used in the delay line for two reasons. The first reason is that the focussing force vanishes to first-order. This effect is plausible if one recalls that orbit diameters of electrons with energies of about 10 ev in fields of the order of kilogauss are much less than a millimeter. On the other hand, magnetic field gradients which are large enough to be effective in producing focussing must persist in the same direction on the average over regions which are centimeters in extent. Therefore, the electrons are continually (every half revolution) reversing their direction with respect to the direction of the gradient, and thus the focussing vanishes to first-order. J. Thibaud has shown that a second-order focussing does occur but it is exceedingly weak.¹ This second-order effect can be understood in the light of the strong focussing theory of Cristofilos² and Courant, Livingston, and Snyder³.

The second reason that magnetic focussing cannot be used is that the gradient itself produces a translational drift velocity similar to that of a crossed electric field. Unlike the electric

1. J. Thibaud, *Il Nuovo Climento* 15, 313 (1938).

2. N. Cristofilos (unpublished).

3. E. D. Courant, M. S. Livingston, H. S. Snyder, *Phys. Rev.*: 88, 1190 (1952); 91, 202L (1953).

case, however, this drift velocity is energy dependent; therefore monoenergetic electron beams would be required for high resolution. These two effects are calculated in Appendix I.

The delay line accordingly uses electric focussing to keep the beam from becoming diffuse. The focussing field and the crossed field are the two perpendicular components of the fringing electric field at the edge of a thin charged plate as shown in Figure 2. These components are calculated in Appendix II. With this arrangement the plane of the plate becomes the preferred plane of motion, and the focussing force is always directed toward this plane. The crossed field parallel to the plane of the plate is by no means uniform, since it approaches a very large value at the edge of the plate. However, at a suitable distance from the edge the field is reasonably linear, and since the elementary circular orbit is so small, the only effect of the electric field gradient is to alter slightly the angular velocity of the electron in the circle. See Appendix I.

It was pointed out in the previous section that the delay time could be easily adjusted by changing the potential of the plate. With the above arrangement the focussing force is also changed, and thus the attenuation of the ~~delayed~~ signal increases as the delay time is increased by decreasing the plate potential. While the delay time depends only on the ratio of the electric to magnetic field, it is clear that the delay line should use as strong a magnetic field as practicable in order that the attenuation be kept small at the maximum delay (smallest electric field) desired.

IV. Experimental Delay Line

Chamber

The vacuum chamber of brass shown in Figures 3 and 4 was 1/2" deep and 3" in diameter. A thin .011" copper disk 2" in diameter was symmetrically placed in and insulated from the chamber. Small Kovar seals placed in the wall permitted connections to be

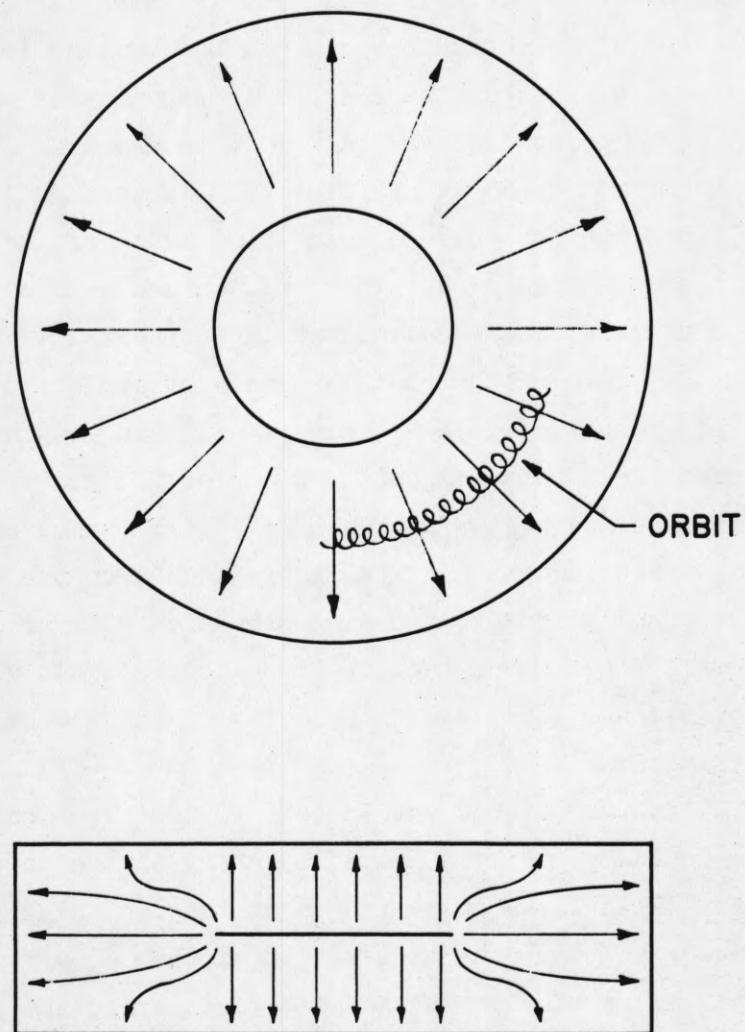


FIG. 2 SCHEMATIC REPRESENTATION OF THE
DELAY LINE FIELD GEOMETRY.

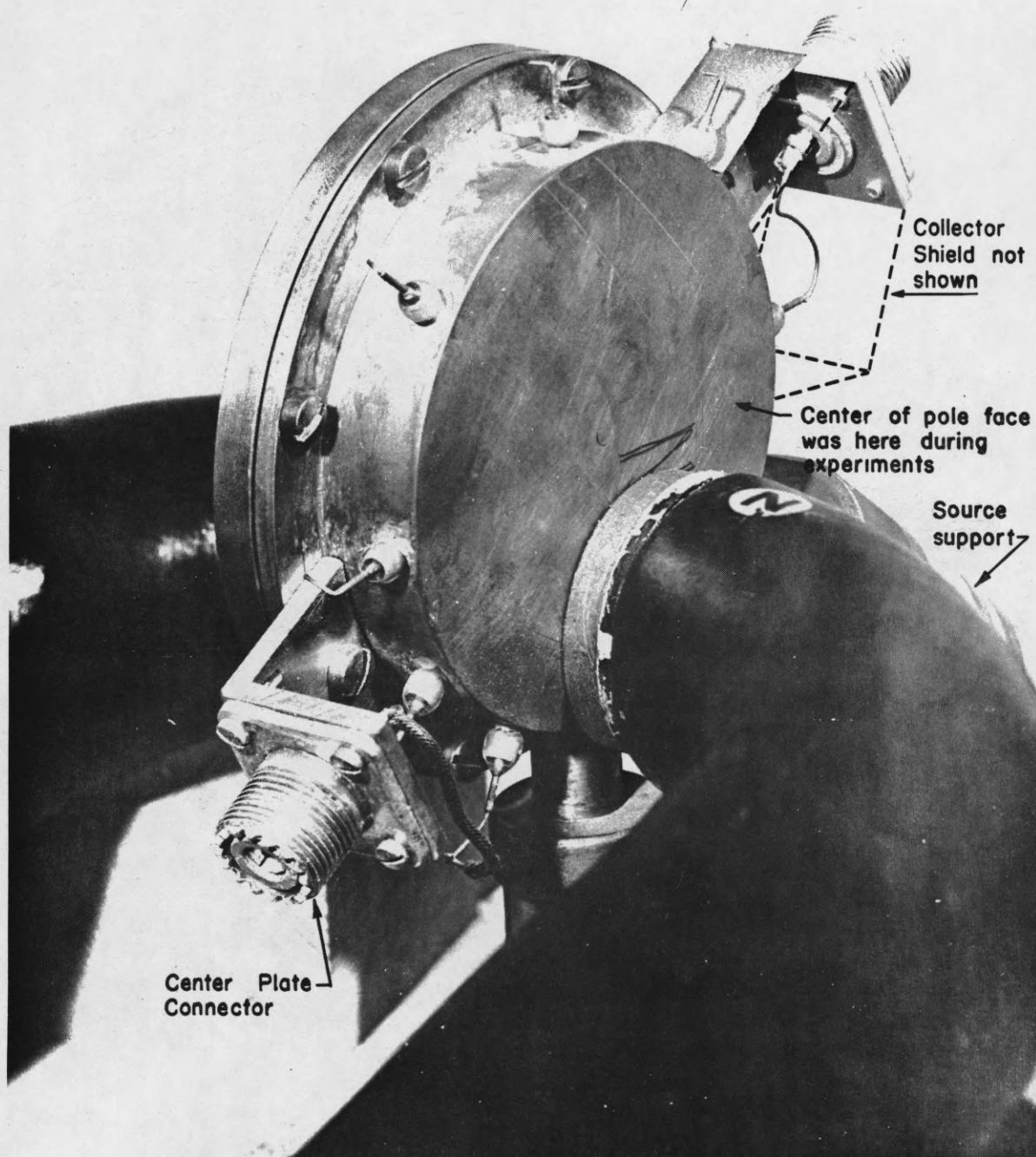


FIGURE 3. EXTERIOR VIEW OF CHAMBER AND MAGNET.

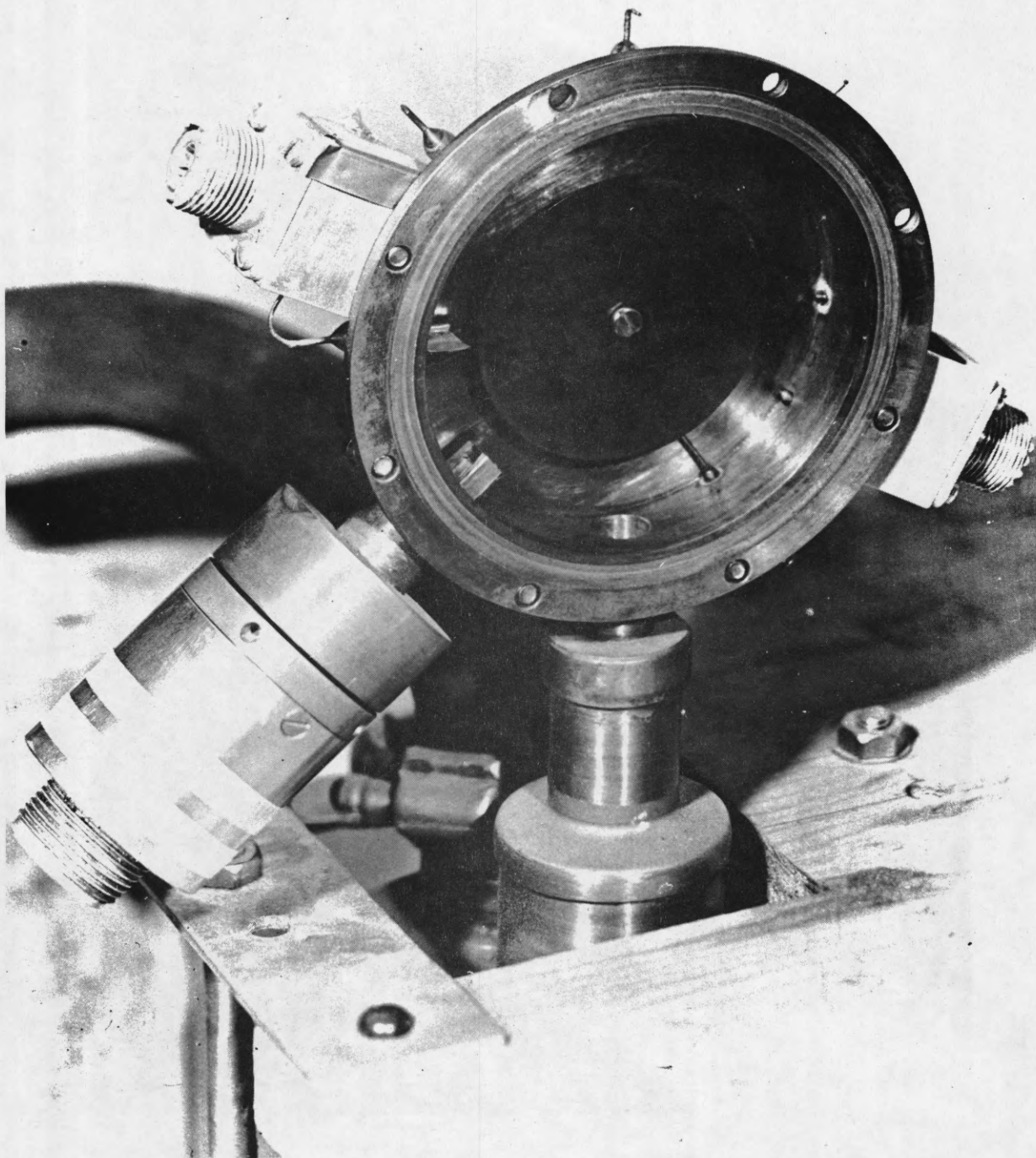


FIGURE 4. CHAMBER INTERIOR.

made to this center plate and to the collector (of copper: $1/4 \times 3/8 \times .004$). The chamber was evacuated by means of a VMF-10-04 DPI air-cooled oil-diffusion pump. No ion or other pressure gauge was used.

Source

The source shown in Figures 4, 5 and 6 was removable and consisted of the filament assembly from a 2.5-3 volt flashlight bulb, a "grid" or puller, and a shield.

The puller was made of .004" copper and in essence was a half cylinder $1/4$ " high and .025" diameter; the stretched-out filament was placed on the axis of this cylinder. Since the axis is parallel to the external magnetic field, the source geometry and behaviour are very similar to that of a split anode magnetron.

The shield was a rectangular box which covered the above combination and had a small rectangular window at one edge.

Figure 7 of the internal geometry should complete this brief description of the apparatus.

Circuit

The potentials of the electrodes could be varied independently as shown in Figure 8. The chamber was at ground potential and all potentials were measured with respect to ground. The galvanometer was used to check the magnitude and polarity of the current to the collector while static properties of the source were being measured. The Ayrton shunt was shorted out during the pulse measurements to avoid introducing pickup in the 1st grid circuit of the preamplifier.

Magnetic Field

The device was designed to be used in a uniform magnetic field, at least uniform over the annular extent between the edge of the center plate and the chamber wall. The Kovar seals were provided to allow the collector to be placed at increasingly greater distances from the source. The chamber was ready to be tested before a suitably uniform magnetic field of sufficient extent and strength was available. Therefore a small magnetron magnet with a $1 \frac{1}{16}$ " gap and $1 \frac{9}{16}$ " diameter pole faces was used.

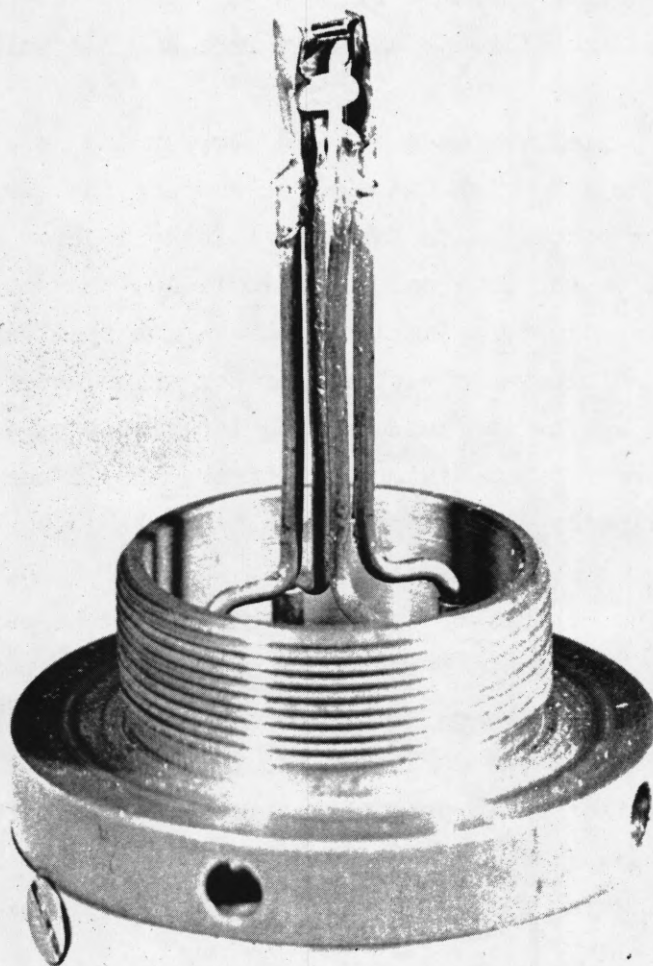


FIGURE 5. SOURCE WITH SHIELD REMOVED.

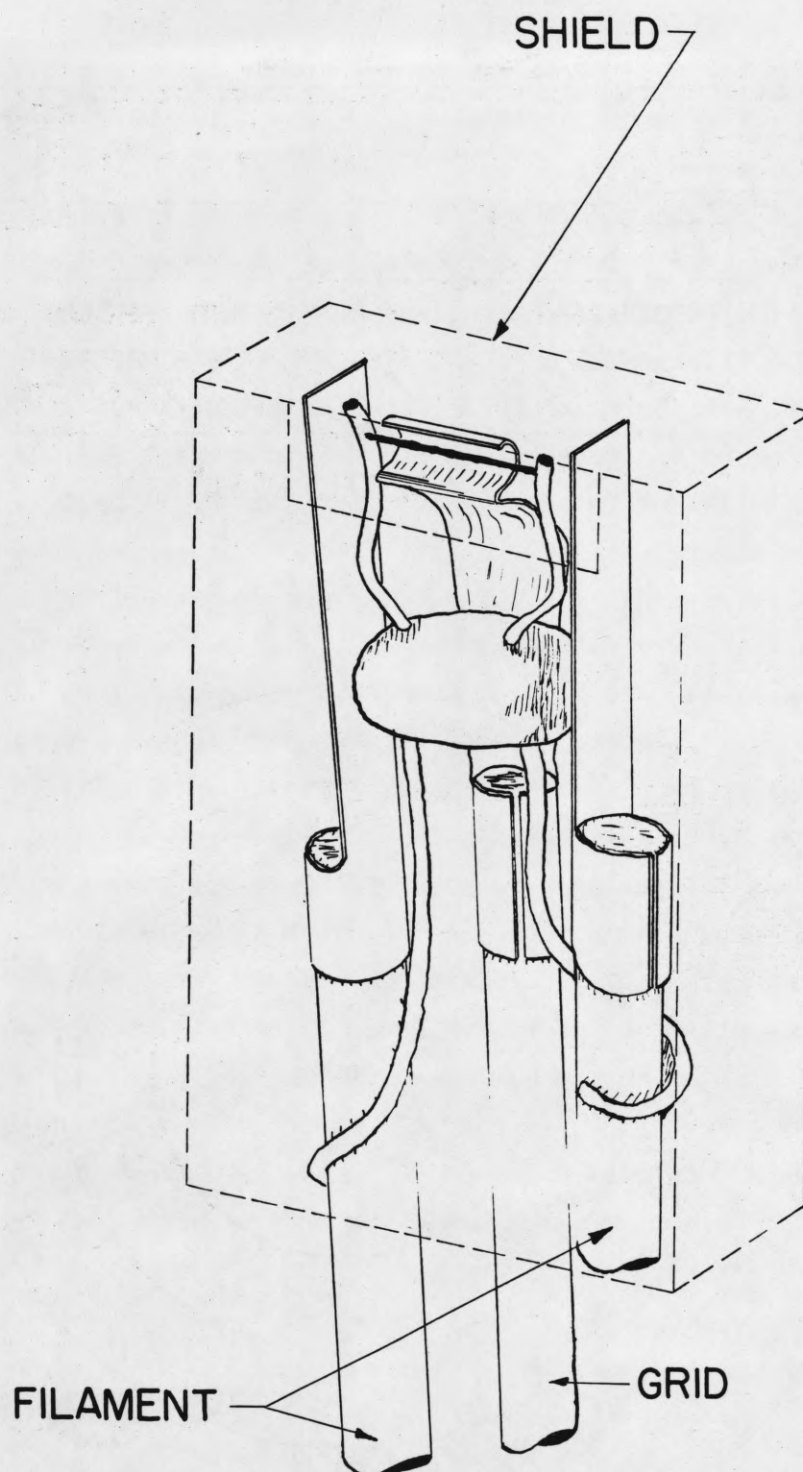


FIGURE 6 SOURCE DETAIL

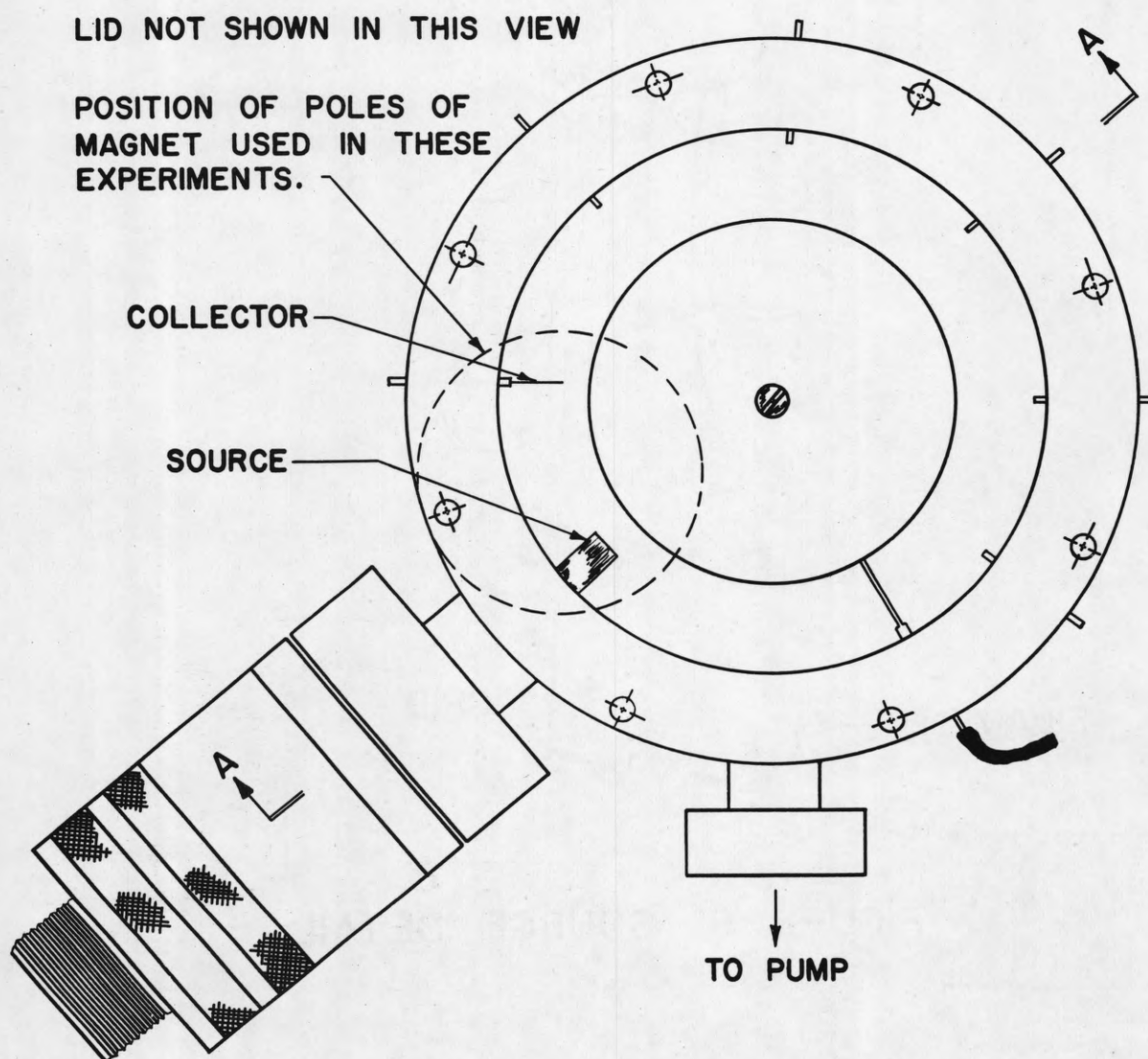
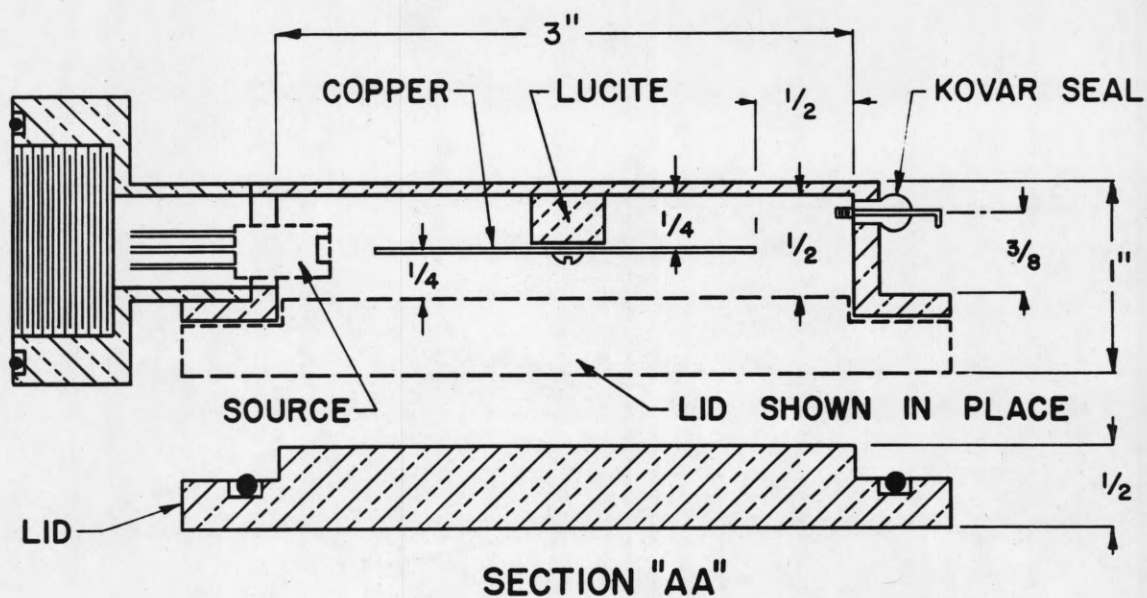


FIGURE 7 CHAMBER DETAIL

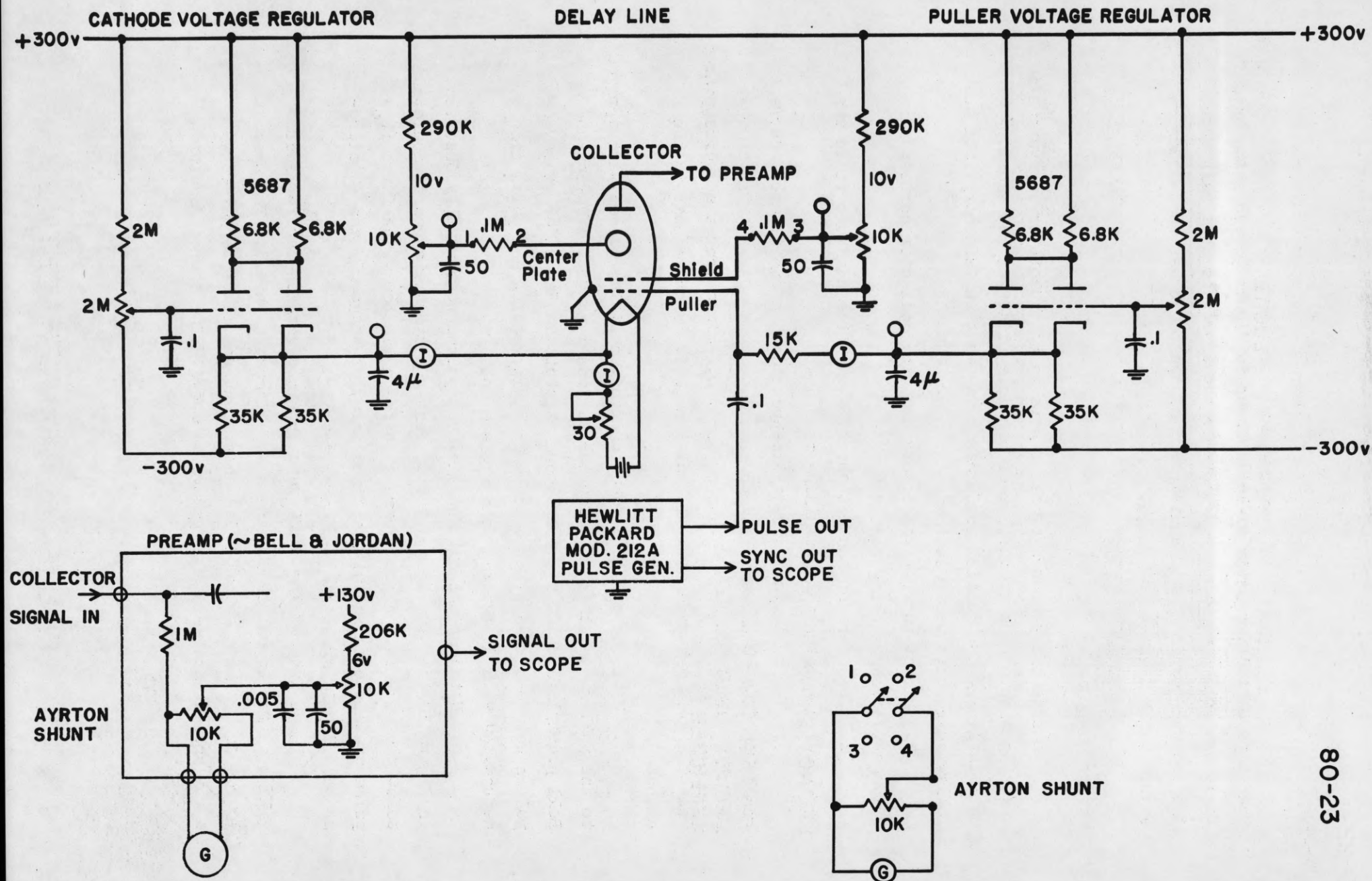


FIGURE 8 CIRCUIT SCHEMATIC

The shape of this magnetic field is shown in Figure 9. In using this field the collector was moved close to the source so that only about the central portion (1 inch diameter) of the field was used. See Figure 7 for location of field.

V. Results

Due to the pressure of other work in the laboratory a systematic investigation of the properties of the delay line was cut short. Qualitatively, the initial performance was most satisfactory, and the following results were obtained:

1. Direct current was observed at the collector corresponding to negative charge being received.

2. This current was not observed when the magnetic field was reversed, all potentials remaining the same.

3. The collector current disappeared when the filament current was dropped below the emission threshold.

4. This current was the order of 0.1 microamperes and disappeared, when the grid was made about 10 volts negative with respect to the cathode.

5. With the puller biased to cutoff positive pulses were applied to the puller, and the collector current observed with a Jordan and Bell preamplifier and a synchroscope as shown in Figure 8. Delayed pulses were observed with the time delay increasing and pulse size decreasing with decreasing center plate voltage.

6. Not just one but four delayed pulses were usually observed. In Figure 10 the time delays versus center plate voltage are tabulated below the wave form of the current to the collector. The first (t_0) pulse usually occurred with a fixed delay of between 3 and 10 microseconds depending on the source potentials.

These data of Figure 10 were obtained with an earlier source with a different puller structure and without a shield. The present source design gave better pulse shapes but the multiple pulses were still present and seemed to behave as above. The source conditions

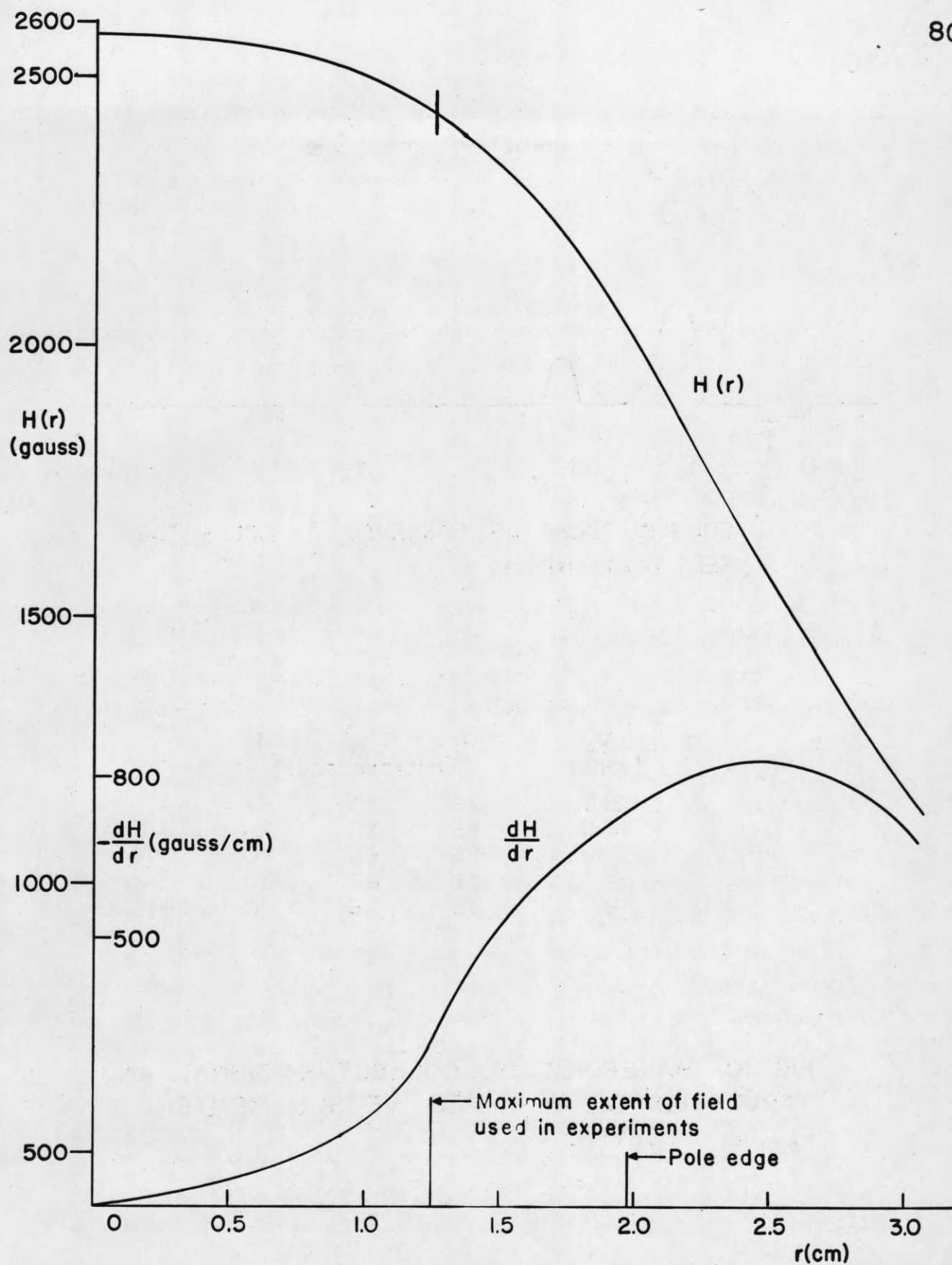
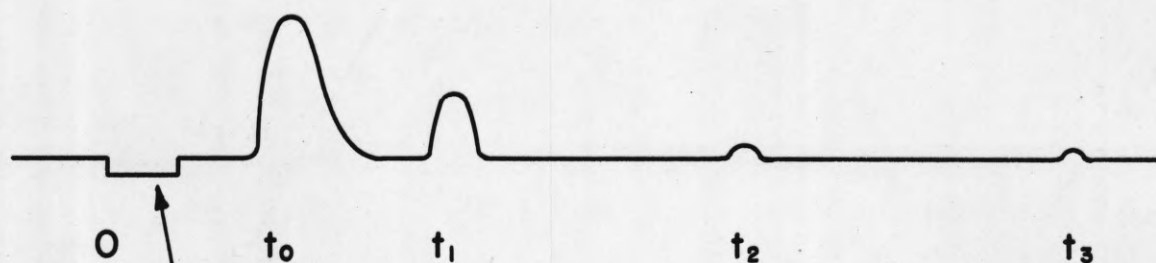


FIGURE 9 RADIAL PLOT OF MAGNETIC FIELD INTENSITY ON MEDIAN PLANE.



SOURCE PULSE AS OBSERVED AT COLLECTOR.
SEE TEXT (8)

V_0 (volts)	t_1 (microseconds)	t_2	t_3
21.5	22	45	67
18.0	25	50	76
15.25	28	60	90
14	31	67	100
12	35	79	>100 (amplitude ~ 0)

FIG. 10 WAVEFORM OF COLLECTOR SIGNAL AND
TABULATED DELAY TIMES VERSUS CENTER
PLATE VOLTAGE.

for these results are:

pulse rate, 600pps; length, $4\mu\text{sec}$; amplitude, +50v;

I fil = 200 ma; I cath = 0 ma; I puller = 0 ma;

V collector = 0 volts; V cath = -25 v; V puller = -12v.

The stability was excellent; one could leave the equipment running, come back an hour later, and find no change in the wave form.

A typical set of potentials for the present source design is V cath = -50v; V puller = -60v; V shield = +8v.

7. With the earlier source mentioned above one occasionally observed under exceedingly critical and transitory conditions a fine structure of pulses within each of the last three pulses. As the center plate voltage was changed, these smaller pulses appeared to slide through each other but still moved along with the behaviour as tabulated above.

8. The impressed signal on the puller was rectangular in shape. This signal was observed by removing the collector shielding external to the chamber as in Figures 3 and 4 and increasing the stray capacity between the collector and the pulse output of the pulse generator. This shows that the rounding and decidedly gaussian shape of the pulses 1, 2, 3 in Figure 10 is real and is not due to time constant effects in the circuits. This impressed signal was positive and was seen to be opposite in sign to the delayed pulses.

VI. Discussion

When the electric and magnetic fields are uniform there is no focussing force to keep the electrons in a beam. By using a disk instead of a cylinder for the center electrode, the electric field between the edge of the disk and the chamber wall has a vertical (z) component parallel to the magnetic field, and when the disk is positive with respect to the chamber, this component provides a vertical focussing force for electrons. For the geometry as described the electric field is to about 20 % (i.e., neglecting curvature of the box and disk and treating the

potential problem as two dimensional as in Appendix II):

$$\begin{aligned} E_x &= 0.348V_0(1 - 2.39x) \\ E_z &= 0.830V_0z \end{aligned} \quad \text{volts/cm}$$

where x is measured from the mid-point of the gap and is positive toward the wall. These expressions are just the first terms of a Taylor expansion of the fields. The only effect of the gradient in E_x is to alter slightly the angular velocity of the electrons in the magnetic field and to make the orbit slightly elliptical in the moving frame of reference. The angular velocity is equal to:

$$(eH/mc)(1 - 2.31V_0/H^2). \quad \text{radians/sec. (Appendix I)}$$

The effect of non-uniformities in the magnetic field is to produce translational drift velocities,

$$v_{yd} = 10^8 (T/H^2)(dH/dx) \quad \text{cm/sec, (Appendix I)}$$

perpendicular to the direction of the magnetic field gradients, where T is the kinetic energy of the particles in electron volts. These velocities vary with the kinetic energies of the particles and so tend to produce a dispersion of the particles, if there is any energy spread in the beam.

To first order, these effects of non-uniformities in the fields are linear and additive. Some unsuccessful attempts have been made to analyze the motion when the extent of the orbit is large enough to require consideration of higher order terms, or the closed expressions for the electric field.

With this much as background information some understanding of the results can perhaps be had. Two questions raise themselves immediately. Are the delayed pulses due to electrons or negative ions? Why are there multiple pulses?

The first question remains unanswered by the results 1 through 4. The particles could be ions, but then the radius of curvature would be increased by the square root of the mass ratio (ion to electron), if the energy of the ions were the same as the electrons; that is, the ions would move in orbits some 40 times larger than the

0.2 mm diameter orbits of 50 volt electrons, i.e., completely out of the orbit region. A comment about 2 is in order. By reversing the sign of the center plate potential the original sense of the drift velocity would be restored, and negative current to the collector presumably could be observed again. But the vertical component of the electric field would now be reversed and there would be a defocussing force on the beam so that no collector current would be possible. This experiment was not tried.

The magnitude of the collector current in 4 is of the same order as the ion current in an ionization gauge with 10^{-5} to 10^{-6} mm pressure, which suggests that the charge transport might be due to negative ions. However, the plate current in an ion gauge is positive, and furthermore, the geometry is considerably different. Perhaps the negative ions are formed in a similar way to those in a Phillips gauge but the delay line source potentials are much lower. On the other hand, an emitting filament increases the probability of electron attachment. Thus the first question remains completely unanswered by the first four results.

The result in 5 suggests that the delay line is functioning as intended since the delay should increase and the pulse size decrease as the center plate voltage is decreased. Both of the effects are due to the electric field decreasing and thereby decreasing the drift velocity and focussing force. This latter result shows that it is desirable to operate the delay line with stronger magnetic fields so that the same delay can be obtained with a stronger electric field and thereby achieve better vertical focussing.

The answer to the second question of multiple pulses is not known either. In Figure 11 the quantity, $10^3/t_1$, is plotted for three groups of pulses. Under the assumption that the particles are electrons this quantity should vary linearly with V_0 as follows.

$$10^3/t_1 = 10^5 E/LH = 5.48V_0$$

where L is the path length (2.54 cm) and E is $0.348V_0$ volts/cm;

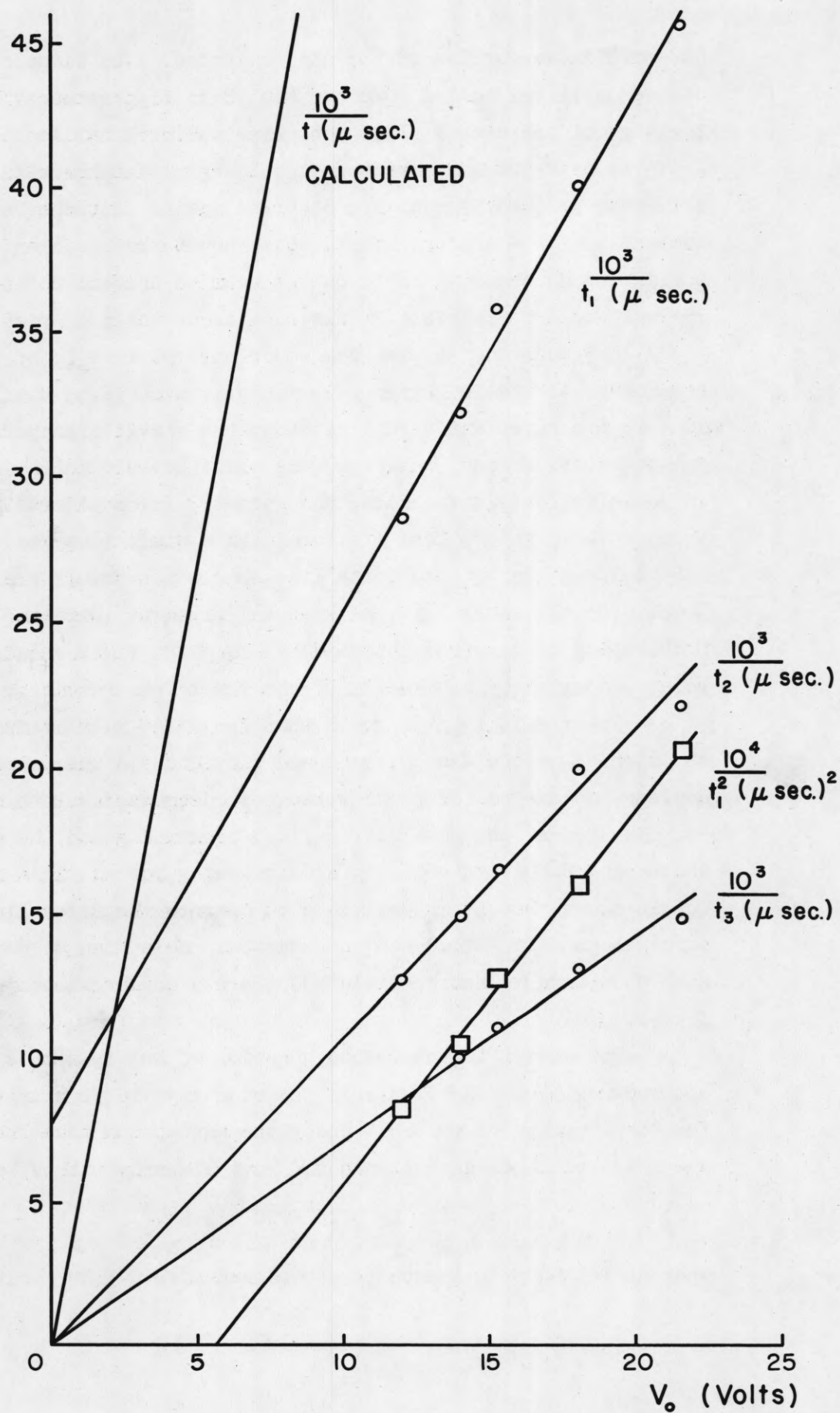


FIGURE II GRAPH OF RESULTS

the steepest line is a plot of this relation. The slope of this expected relation is 3.1, 5.1 and 7.6 times bigger than the slopes of the t_1 , t_2 , and t_3 lines, respectively, which implies that the particles are moving slower than expected or that the path length is somehow longer than the source-to-collector distance. Disregarding the second and third pulses for the moment, the disagreement by a factor of three is not too difficult to account for. The approximation of the electric field by neglecting the curvature of boundaries should introduce an error of the order of $\Delta r/r$ or about 20 %/o. The small magnetron magnet was measured with a G. E. gaussmeter which should be good to 5 %/o. The path length, assuming it to be an arc of a circle, might be 10 to 20 %/o longer, if the beam is close to the wall. The electric field at the wall is about $1/2.5$ that at the mid-point ($x = 0$) of the gap. Putting these together it seems that the t_1 line can be brought into agreement by assuming the particles to be moving close to the wall.

Another possibility is that the path is not a simple arc, but it is difficult to visualize a path that is three times longer than that assumed. Such a path might be a sinusoid about the simple arc, but there is nothing in the first order equations of motion that indicates any tendency for the mean position of the particle to oscillate about a stable orbit.

A curious fact is to be noted in the data tabulated in paragraph 6 of the results. The arrival times of the t_2 and t_3 pulses are almost exactly 2 and 3 times, respectively, the arrival time of the t_1 pulse for any center plate potential. One explanation may be that the arrival of the first pulse somehow is able to impress a large enough signal on the "puller" to initiate another pulse and so on, thus producing a series of equally spaced pulses. Such an explanation ignores the fact that the shielding between the collector and puller circuits is very good and that the pulser is a low impedance generator.

It has been suggested that perhaps the multiple pulses were due to recirculation around the entire chamber by the first

pulse. If the effect of the radial magnetic field gradients is ignored, and if the magnetic field is assumed to drop immediately to a low value for the entire (7 times longer) path from collector to source, and if the data of Figure 10 is used to obtain an estimate of the time to traverse this portion of the path, the orbit diameters in this external region turn out to be anywhere from 3 cm to 1/2 cm and thus this mechanism may be the cause of the multiple pulses.

Another explanation might be that the current to the collector is due to negative ions and that by a Phillips-type process the source produces multiply charged ions. These ions may have a spectrum of kinetic energies depending on where and how they are produced. If the ions are produced with sufficiently low energies such that the elementary orbit diameters are of the same order as those of electrons, then the motion of the ions is essentially that in crossed fields, and therefore the motion is independent of charge. Thus these low energy multiply charged ions cannot account for the occurrence of multiple pulses.

If the ions are produced at potentials comparable to the electrons leaving the cathode, the orbit radii will be $\sqrt{M/mZ}$ times the corresponding electron orbit radius, where M/m is the ion to electron mass ratio and Z is the valence state of the ions. For O^{+} , as an example, this represents a factor of about 120 or a radius of about one centimeter assuming a potential of 50 volts. If the radii are this large, being comparable with the path length, then one can, as a very crude approximation, neglect the presence of all the fields and ask what is the relationship between the time of the arrival of multiply charged ions which have fallen through the same potential difference. It is easy to show that the time of arrival varies, in this case, inversely as the square root of the valence state of the ion. Thus, multiply charged ions are a dubious source of this integral relationship among the arrival times. (The ratio of the charges would have to 36:9:4.) Moreover, it is difficult, using ions as the means for charge transport, to understand how the center plate potential can effect the delay time.

That is, under these assumptions the delay time should be independent of the center plate voltages. This mechanism may account for the large broad t_0 pulse shown in result 6.

As a wild hypothesis, still assuming multiply charged ions, but overlooking their failure to explain the integer relationship, one can try to use the center plate potential as the acceleration potential. This gives for the arrival time

$$t = \frac{L}{v} = \frac{L}{c} \sqrt{\frac{Mc^2}{2ZeV_0}} = \frac{L}{c} \sqrt{\frac{m_p c^2 A}{2eV_0 Z}}$$

This relation has also been plotted in Figure 11 for the t_1 pulse and surprisingly enough seems linear between $10^4/t_1^2$ and V_0 . Using the slope, one obtains an average value of 2350 for A/Z , the atomic weight to valence ratio, which suggests approximate molecular structures as $(CH_2)_{168}$.

In summary it seems likely to presume the pulses to be due to electrons, as too many difficulties are encountered if one tries to explain the facts with ions. It is quite possible that the effect of non-uniformities in the electric and magnetic fields cannot be approximated with a simple linear treatment. The gaussian shape of the pulses in 8 for example is probably due to the divergence of the beam in and near the source so that the orbits of the electrons in the beam are at different radii, hence in different electric fields, and hence travel with different drift velocities. Perhaps using a more sophisticated treatment one could show that multiple pulses at integral spacings are to be expected and that the slope of $1/t$ versus V_0 lines does agree with the data.

In any future experimental work a more uniform magnetic field and a much better vacuum should be used. The latter should provide a decisive answer to the ion question, and the former may remove the multiplicity of pulses.

Appendix I.

Motion of a Charged Particle in Various Static Fields

Uniform Magnetic Field

By equating the inertial and Lorentz forces on an electron the vector equation of motion is obtained,

$$\ddot{\underline{r}} = \underline{\omega} \times \dot{\underline{r}} \quad , \quad \underline{\omega} = e\mathbf{H}/mc.$$

This equation has the well-known solution of a helical orbit, or if there is no velocity component parallel to the field direction, the orbit is circular. In vector form this latter solution may be written in the compact form, $\underline{r} = \underline{r}_0 + \underline{a}$, where \underline{r} is the vector specifying the location of the electron, \underline{r}_0 is the constant vector specifying the center of the orbit, and \underline{a} is a vector of constant length, a , rotating in a plane perpendicular to \mathbf{H} or $\underline{\omega}$, with angular velocity, $\underline{\omega}$, such that $\dot{\underline{a}} = \underline{\omega} \times \underline{a}$.

Uniform Electric and Magnetic Fields

The addition of a uniform electric field, \mathbf{E} , modifies the equation of motion of an electron as follows:

$$\ddot{\underline{r}} = \underline{\omega} \times \dot{\underline{r}} - (e/m)\mathbf{E}.$$

The solution for this equation is to be found in standard text-books on electricity and magnetism. It is,

$$\underline{r} = \underline{r}_0 + \underline{a} + \underline{v}_d t, \quad (\underline{v}_d \text{ constant}),$$

where it has been assumed that \mathbf{E} and \mathbf{H} are at right angles, and that the motion is again confined to lie in a plane. By direct substitution in the equation of motion we have,

$$\underline{\omega} \times (\underline{\omega} \times \underline{a}) = \underline{\omega} \times (\underline{\omega} \times \underline{a} + \underline{v}_d) - (e/m)\mathbf{E},$$

or

$$\underline{\omega} \times \underline{v}_d = (e/m)\mathbf{E}.$$

Let

$$\underline{\omega} = (eH/mc)\underline{k},$$

where \underline{k} is a unit vector in the direction of \mathbf{H} , i.e. $\mathbf{H} = H\underline{k}$.

Then,

$$\frac{eH}{mc}(\underline{k} \times \underline{v}_d) \times \underline{k} = \frac{e}{m} \underline{E} \times \underline{k},$$

and expanding the double cross product and using the hypothesis, $\underline{v}_d \cdot \underline{k} = 0$,

$$\underline{v}_d = \frac{e}{H} \underline{E} \times \underline{k}.$$

Thus the electron orbit is a trochoid, a pure rotation plus a pure translation perpendicular to the electric and magnetic fields.

It is important to note that this vector expression for the translational drift velocity, \underline{v}_d , is independent of the sign and magnitude of the charge of the particle as well as the mass and kinetic energy of the particle.

The units to be used in the equation of motion are mixed cgs: \underline{r} in cm/sec, $\underline{\dot{r}}$ in cm/sec², H in gauss, E in statvolts/cm, m in grams, and e in esu. With E in volts/cm, H in gauss, the drift speed in cm/sec is

$$v_d = 10^8 E/H.$$

The radius of the circular orbit in the two cases of motion just considered is found most easily by going back to the equation of motion for the magnetic case and expressing it in the scalar form, $mv^2/a = evH/c$ where v is the linear speed of the particle in the path. Since only non-relativistic energies are being considered, this scalar relation may be solved for "a" in cm as follows,

$$a = \sqrt{T 2mc^2} / 300H,$$

where T is the kinetic energy of the electron expressed in electron volts (ev), and mc^2 is the rest energy of the electron in ev (for the accuracies of this experiment $2mc^2$ is 10^6 ev), and H is in gauss. Thus an electron that has been accelerated through a potential difference of 100 volts will have a kinetic energy of 100 ev and will have an instantaneous speed in the path,

$$v = 6 \times 10^7 \sqrt{T} = 6 \times 10^8 \text{ cm/sec},$$

and in a magnetic field of 3,300 gauss will have an orbit radius of 0.1 mm.

Non-Uniform Static Magnetic Field

When the magnetic field is not quite uniform the electron will follow an orbit that is almost circular. The motion can be regarded as

being trochoidal on the average; that is, the center of the circular orbit is translated at a rate which, on the average, is proportional to the non-uniformity in the field. A crude explanation of the source of the drift motion is that during half of a revolution the electron is in a weaker field and is moving in a greater than average radius circle, whereas in the next half revolution the electron moves in a smaller circle as a consequence of the stronger field.

Expressed in another way, the motion can be regarded as circular with the addition of a perturbation arising from the field inhomogeneity. Thus ω can no longer be regarded as constant but only nearly so. Expanding $\omega(\underline{r})$ in a Taylor series about the average orbit center \underline{r}_0 ,

$$\omega(\underline{r}) = \omega(\underline{r}_0) + \Delta \underline{r} \cdot \nabla \omega.$$

Upon substituting in the equation of motion as follows,

$$\ddot{\underline{r}} = \omega(\underline{r}_0) \times \dot{\underline{r}} + (\Delta \underline{r} \cdot \nabla \omega) \times \dot{\underline{r}},$$

it is seen that the additional term on the right-hand side can be regarded as being equivalent to a fictitious electric field*. Therefore it is reasonable to suppose that the motion will resemble the motion in crossed fields which was treated above. Since, $\Delta \underline{r} = \underline{r} - \underline{r}_0 + \underline{a} + \text{small terms of the order of } \nabla \omega$, it is clear that the motion in this case cannot agree in detail with the crossed field case, because the fictitious field term is periodic in time i.e. it vanishes every time $\Delta \underline{r}$ is perpendicular to the direction of the field gradient. However, since the average of the perturbing term over one revolution of the electron is a non-vanishing vector, the average solution of the equation of motion to first order can be expected to be exactly that given in the crossed field case.

The motion is visualized to occur in a plane perpendicular to the main direction of the field such as the median plane in the air gap of a magnet. The median "plane" is that surface, usually symmetrically located between the poles of a C-shape magnet, such that the field is everywhere perpendicular to it. Let the field direction be specified

* H. Alfvén, Cosmical Electrodynamics

by the unit vector, \underline{k} , let $\underline{\omega}(\underline{r})$ be written as $\omega(\underline{r})\underline{k}$, and denote $\omega(\underline{r}_0)$ by ω . To first order the perturbing term in the equation of motion is,

$$(\underline{a} \cdot \nabla \omega) \underline{k} \times (\omega \underline{k} \times \underline{a})$$

Expanding the double cross product and using $\underline{a} \cdot \underline{k} = 0$, the term becomes,

$$- \omega (\underline{a} \cdot \nabla \omega) \underline{a}$$

The average of this term over one revolution of \underline{a} is,

$$- \frac{1}{2} \omega a^2 \nabla \omega$$

Regarding this term as the electric field term in the crossed field case, the drift velocity is given by,

$$\omega \underline{k} \times \underline{v}_d = + \frac{1}{2} \omega a^2 \nabla \omega$$

or

$$\underline{v}_d = + \frac{1}{2} a^2 (\nabla \omega) \times \underline{k}$$

Expressed in terms of the field quantities and the kinetic energy, T , in ev the magnitude of \underline{v}_d in cm/sec is,

$$v_{dy} = \frac{1}{2} 10^8 \frac{T}{H^2} \frac{dH}{dx}.$$

Unlike the crossed field case, however, this drift velocity is energy dependent and therefore the presence of inhomogeneities in the magnetic field will react with the natural energy spread in the electron beam to produce a dispersion in drift velocity, which effectively cuts the bandwidth of the delay line.

Before proceeding directly to treat the vertical motion (parallel to the field) an outline of a complete analysis of the motion for the case of the usual magnetic field to be found in air gaps will be given. The advantage of such a digression is that it shows the analogy of the present small radius motion with the large radius motion found in particle accelerators such as the betatron and the cyclotron. In such machines the field is usually taken to be a function only of the distance, r , from the field center and the distance, z , from the median plane. The field measurements usually yield the field strength on the median plane, $H_z(r, 0)$. Using the properties of the field in the gap, the radial component must

vanish on the median plane, the divergence and the curl must vanish, the field in the neighborhood of the radius, r_0 , can be written as,

$$\underline{H}(r,z) = z D_0 \underline{\underline{e}} + H_0 \underline{k} + (r-r_0) D_0 \underline{k},$$

where $\underline{\underline{e}}$ is the radial unit vector, $H_0 = H_z(r_0, 0)$, and D_0 is the derivative of $H_z(r,0)$ with respect to r evaluated at $(r_0, 0)$.

It is conventional to describe the dependence of the field on r in the neighborhood of r_0 by the index, n ; that is,

$$H_z(r,0) = H_0 (r_0/r)^n,$$

so that

$$D_0 = -H_0 (n/r_0).$$

The position of the particle is described by the vector,

$$\underline{r} = \underline{a} + \underline{b} + z \underline{k},$$

where \underline{a} as before describes the largest part of the motion, $\underline{a} \cdot \underline{k} = 0$, \underline{b} corresponds to the $\underline{v}_d t$, $\underline{b} \cdot \underline{k} = 0$, and \underline{b} is taken to vanish. Then,

$$\Delta \underline{r} = \underline{r} - \underline{r}_0 = \underline{a} + \underline{b} - \underline{r}_0 + z \underline{k}$$

is the vector describing the displacement of the particle from the radius \underline{r}_0 . Writing the magnetic field in the compact form $\underline{H}(\underline{r}) = H_0 \underline{k} + \Delta \underline{r} \cdot \nabla H$, it is seen that the tensor, $\nabla H = D_0 (\underline{k} \underline{\underline{e}} + \underline{\underline{e}} \underline{k})$, will yield radial and vertical components when the scalar product with $\Delta \underline{r}$ is taken. Letting ω_0 be (eH_0/mc) , substituting into the equation of motion and separating radial and vertical components the following first order equations are obtained

$$\underline{k} \times \dot{\underline{b}} = -W_0 (\underline{b} + \underline{a} - \underline{r}_0) \cdot \underline{\underline{e}} \underline{k} \times (\underline{k} \times \underline{a})$$

$$\dot{z} \underline{k} = \omega_0 W_0 z \underline{\underline{e}} \times (\underline{k} \times \underline{a})$$

where W_0 is (eD_0/mc) . The second-order terms, $\Delta \underline{r} \cdot \nabla \omega \times \underline{b}$ and $\Delta \underline{r} \cdot \nabla \omega \times z \underline{k}$, have been neglected, because $\dot{\underline{b}}$ and \dot{z} are both of the order of $\nabla \omega$ which is presumed to be small. Two cases can now be distinguished. The first is the small radius motion that this report is principally concerned with. The second is the cyclotron and betatron case. In the first case $\underline{b} = \underline{r}_0$ but \underline{r}_0 can slowly rotate. This gives for the drift velocity in the

median plane,

$$\langle \dot{\underline{b}} \rangle = \langle \dot{\underline{r}}_0 \rangle = \frac{1}{2} a^2 W_0 \underline{\xi} \times \underline{k}$$

in complete agreement with the previous solution got by analogy with the crossed field case. The vertical equation of motion in this first case can be reduced to the following,

$$\ddot{z} = (\underline{a} \cdot \underline{\xi}) \omega_0 W_0 z$$

The average of the scalar product over one turn of \underline{a} in this case vanishes, and therefore there is no vertical focussing to first-order. Since the spring constant is periodic, however, the results of strong focussing theory can be invoked and focussing therefore does occur. Unlike the usual case in the strong focussing theory the field gradient term is not large but small, and therefore this second-order magnetic focussing is weak. Moreover, it is undesirable to have magnetic gradients, because of the deleterious effect on resolution in the delay line.

Turning now to the second case, that of large radius motion found in large machines, the assumption is that $\underline{a} = \underline{r}_0$. Direct substitution of this yields,

$$\underline{k} \times \dot{\underline{b}} = + (\underline{b} \cdot \underline{\xi}) W_0 \underline{a}$$

An interpretation of the scalar product must now be made; this product is the displacement of the particle from the equilibrium orbit, and therefore $\underline{\xi}$ rotates with \underline{a} , that is

$$\underline{\xi} = \underline{a}/r_0$$

Thus,

$$\underline{k} \times \dot{\underline{b}} = + (\underline{b} \cdot \underline{a}) W_0 \underline{a}/r_0$$

Averaging,

$$\langle \dot{\underline{b}} \rangle = \frac{1}{2} r_0 W_0 \underline{b} \underline{\xi} \times \underline{k},$$

where $\underline{b} = b \underline{\xi}$, since \underline{b} is a radial vector also but does not turn as rapidly as \underline{a} . The average angular velocity of \underline{b} is $\langle \dot{\underline{b}} \rangle/b$ and is denoted by ω_c . For the case of usual fields encountered in air gaps, the sense of ω_c is the same as the sense of ω_0 , the angular speed of the particle in an equivalent uniform field. When the two vectors \underline{a} and \underline{b} are rotating in the same sense, the angular frequency of the radial oscillation is $\omega_0 - \omega_c$ or in terms of the field index, n , this becomes $\omega_0(1 - n/2)$. This

approximate relation, obtained by averaging procedures, is to be compared with the precise first-order treatment which gives for the radial angular oscillation frequency $\omega_0 \sqrt{1-n}$, which for small n is approximately $\omega_0 (1 - n/2)$ as above.

The vertical case in large radius motion, with $\underline{a} = \underline{r}_0 = r_0 \underline{\hat{e}}$, and in terms of the field index becomes the familiar harmonic oscillator,

$$\ddot{z} = -\omega_0^2 n z$$

whose angular frequency is $\omega_0 \sqrt{n}$. Thus it is seen that this single perturbation method yields the correct average solutions in inhomogeneous fields for both small and large radius motions.

Uniform Magnetic Field and Crossed Non-Uniform Electric Field

The electric field in the orbit region of the delay line is given in Appendix II. When this is used in the equation of motion and taking $\underline{r} = x\underline{i} + y\underline{j} + z\underline{k}$, the component equations of motion can be written as follows,

$$\ddot{x} = -\omega_0^2 y - (e/m) 0.348V_0 (1-2.39x)$$

$$\ddot{y} = \omega_0^2 x$$

$$\ddot{z} = - (e/m) 0.830V_0 z$$

When the second equation is integrated once and \dot{y} substituted into the first equation the result is

$$\ddot{x} = -(\omega_0^2 - (e/m) 0.348V_0 2.39) x + \text{const.},$$

i.e., a harmonic oscillator with a constant forcing term. This latter term shifts the equilibrium position of the oscillator. The angular frequency is the square root of the coefficient of $-x$ and this has the value $\omega_0 (1 - 2.31 V_0/H^2)$ which for all purposes in this experiment is ω_0 .

Appendix II.

Calculation of the Electric Field

The following calculation derives approximate expressions for the two components of the electric field intensity in the neighborhood of the plane of symmetry in the two dimensional configuration shown in Figure 12. This configuration is, of course, an approximation to the actual situation. The effect of the curvature has been neglected. The usual argument is that the $1/r$ term in Laplace's equation in cylindrical coordinates is negligible when the region of interest, Δr , is small compared to r , the distance to the axis. In the case of the model delay line a typical dimension in the region of the orbit is $1/4$ inch, r is about $5/4$ inch, and certainly 20 % is not small.

An approximate solution of a charged disk in a cylindrical box has recently been published* and it should be used in any future work on the delay line. To compare this solution with the approximate solution to be derived involves considerably numerical calculation which will not be undertaken at this time.

Owing to the symmetry of the problem it is only necessary to map half of the region using the Schwarz-Christoffel transformation shown in Figure 13. This transformation maps the interior of the semi-infinite strip of the z -plane onto the upper half of the w -plane. The capital letters denote corresponding points on the boundary. The arrows denote the direction in which the boundary is traversed. The letter A denotes the point at infinity.

Using the second form of No. 126b in Peirce's Tables this differential relation may be integrated. The constants may be evaluated by noting that $w = 0$ when $z = 0$, and $w = 1$ when $z = ib$, and then using No. 664 in the tables the connection between z and w becomes,

$$w = -\sinh^2(\pi z/2b)$$

The problem has now been reduced to that of two semi-infinite coplanar sheets separated by a distance $a' = \sinh^2(\pi a/2b)$ charged to $V_0/2$ and $-V_0/2$, respectively. This problem is solved in Smythe,

* W. R. Smythe, J. Appl. Phys. 24, 773 (1953).

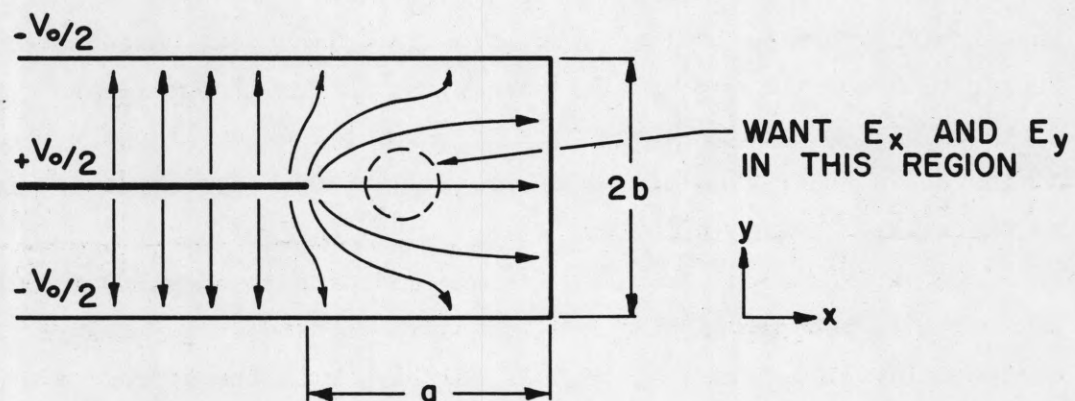
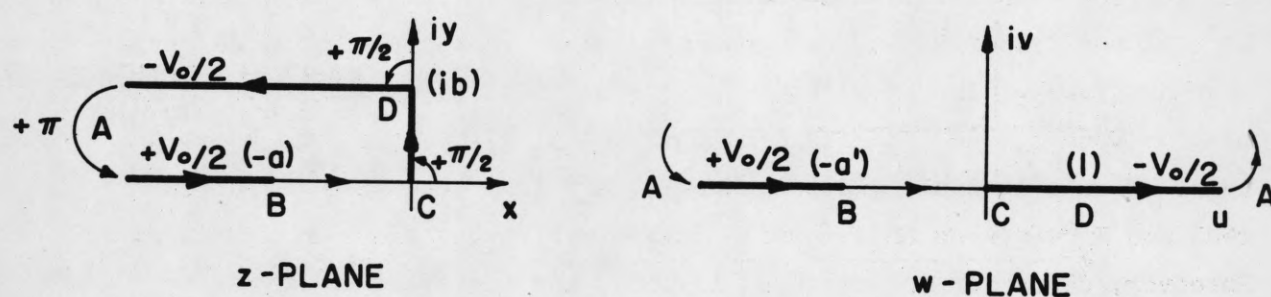


FIGURE 12 TWO DIMENSIONAL REPRESENTATION
OF CHAMBER.



$$\frac{dz}{dw} = \frac{c_1}{w^{1/2} (w-1)^{1/2}}$$

FIGURE 13 MAPPING OF THE CHAMBER INTERIOR
ON THE UPPER HALF-PLANE.

Static and Dynamic Electricity 4.22(3). The solution is:

$$w = -a'(1 + \sin \pi W/V_0)/2$$

where W is the complex potential and $\text{Re}W$ is the potential function. Then the complex electric intensity is,

$$-\frac{dW}{dz} = \frac{V_0}{b} \frac{\cosh(\pi z/2b)}{\sqrt{\sinh^2(\pi a/2b) - \sinh^2(\pi z/2b)}}$$

Before proceeding to evaluate E_x and E_y it is interesting to see the correct behavior of the electric intensity on the boundary. When z is real and less than $-a$, the boundary is the center plate and dW/dz is pure imaginary. Therefore $E_x = 0$, and the field is normal to the center plate. When $z = -a$, the field becomes infinite, as it should be at an edge. When z is real, greater than $-a$, and less than zero, dW/dz is real and E_y vanishes as it should in the gap on the plane of symmetry. Moreover, dW/dz remains real, E_y is zero, and the field is normal to the wall, when z is pure imaginary and less than ib . When $z = ib$, $dW/dz = 0$, and the field vanishes, as it should at an inside corner. When $z = x + ib$ and x is negative, it can be shown that dW/dz is pure imaginary, so that $E_x = 0$, and the field is normal to the conductor, as it should be. Moreover, when x becomes negative and large, dW/dz approaches iV_0/b , the correct limiting value.

The complex electric intensity can be separated into real and imaginary parts but the expressions are very cumbersome. Some simplification can be achieved if y is restricted to be small. The results are:

I (between the edge and the wall) ($-a < x < 0$)

$$E_x = \frac{V_0}{b} \frac{\cosh(\pi x/2b)}{\sqrt{\sinh^2(\pi a/2b) - \sinh^2(\pi x/2b)}}$$

$$E_y = \frac{V_0}{b} \frac{\pi y}{2b} \frac{\sinh(\pi x/2b) \cosh^2(\pi a/2b)}{\sqrt{(\sinh^2(\pi a/2b) - \sinh^2(\pi x/2b))^{3/2}}}$$

II (over the center plate) ($x < -a$, $y > 0$)

$$E_x = \frac{V_o}{b} \frac{\pi y}{2b} \frac{1}{(\sinh(\pi x/2b))^2}$$

$$E_y = \frac{V_o}{b} \operatorname{ctn}(\pi x/2b)$$

This latter result is shown for the sake of completeness, since the particles move only in the first region.

The plot in Figure 14 shows the magnitudes of the two components of the fringing field on a surface 1 mm above the plane of symmetry with $V_o = 10$ volts and $a = 2b = 2.54/2 = 1.27$ cm.

In the orbit region it is seen that the fields are fairly linear. Expanding to order x at the mid-point and using $a = 2b = 1.27$ cm, the fields in the orbit region are

$$E_x(x,y) = .348 V_o (1 - 2.39x) \text{ volts/cm,}$$

$$E_y(x,y) = + .830 V_o y (1 - 3.03x) \text{ volts/cm,}$$

where x is measured from the mid-point and is positive toward the wall.

The y -component of the electric field is in the direction of the magnetic field and has been designated, therefore, as the z -component in the body of this report and in Appendix I.

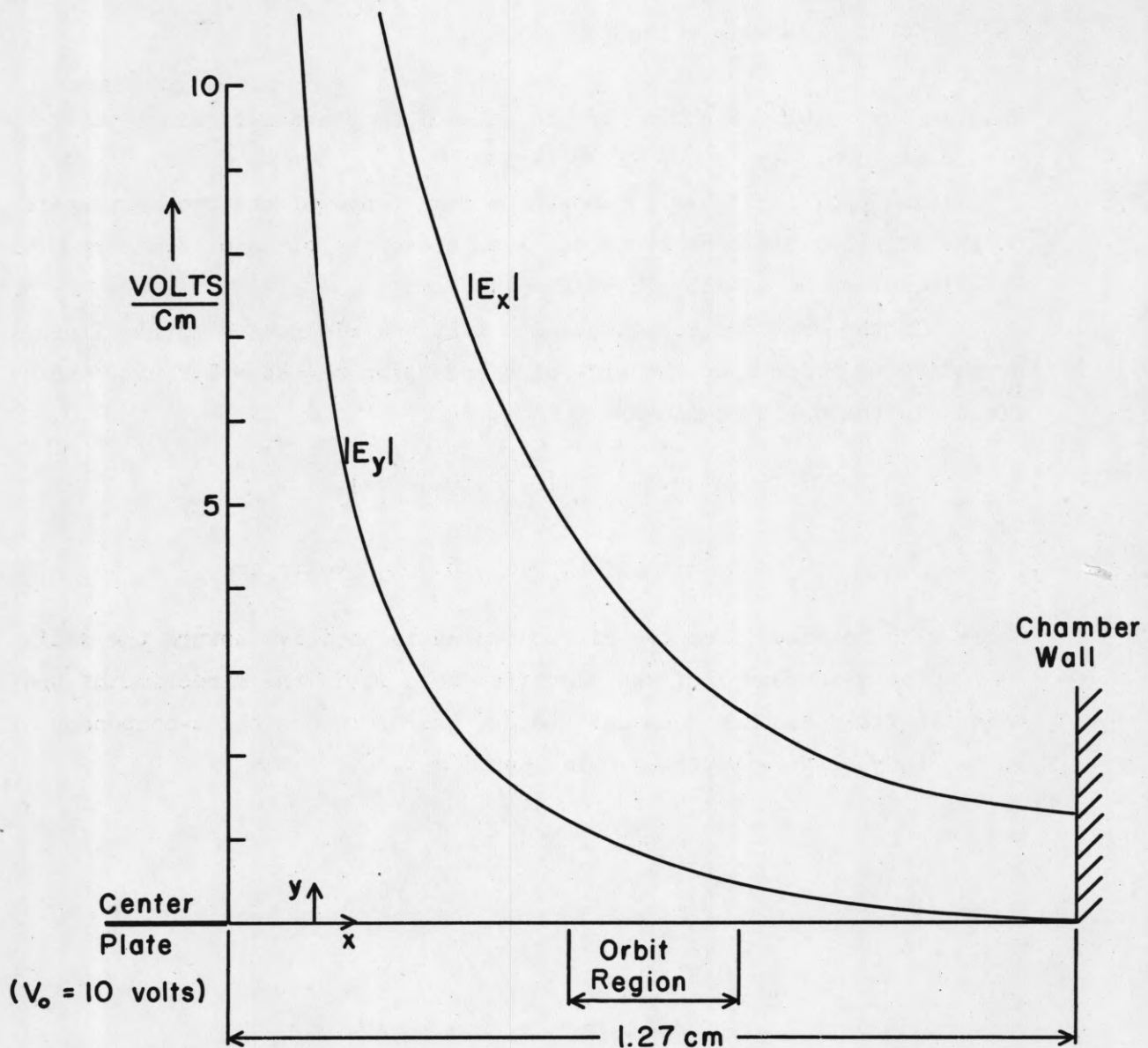


FIGURE 14 PLOT OF THE COMPONENTS OF THE FRINGING FIELD ON A PLANE 1mm. ABOVE THE CENTER PLATE.